

## Van Allen Probes observation of localized drift resonance between poloidal mode ultra-low frequency waves and 60 keV electrons

S. G. Claudepierre,<sup>1</sup> I. R. Mann,<sup>2</sup> K. Takahashi,<sup>3</sup> J. F. Fennell,<sup>1</sup> M. K. Hudson,<sup>4</sup> J. B. Blake,<sup>1</sup> J. L. Roeder,<sup>1</sup> J. H. Clemmons,<sup>1</sup> H. E. Spence,<sup>5</sup> G. D. Reeves,<sup>6</sup> D. N. Baker,<sup>7</sup> H. O. Funsten,<sup>6</sup> R. H. W. Friedel,<sup>6</sup> M. G. Henderson,<sup>6</sup> C. A. Kletzing,<sup>8</sup> W. S. Kurth,<sup>8</sup> R. J. MacDowall,<sup>9</sup> C. W. Smith,<sup>10</sup> and J. R. Wygant<sup>11</sup>

Received 23 July 2013; revised 19 August 2013; accepted 19 August 2013; published 6 September 2013.

[1] We present NASA Van Allen Probes observations of wave-particle interactions between magnetospheric ultra-low frequency (ULF) waves and energetic electrons (20–500 keV) on 31 October 2012. The ULF waves are identified as the fundamental poloidal mode oscillation and are excited following an interplanetary shock impact on the magnetosphere. Large amplitude modulations in energetic electron flux are observed at the same period ( $\approx 3$  min) as the ULF waves and are consistent with a drift-resonant interaction. The azimuthal mode number of the interacting wave is estimated from the electron measurements to be  $\sim 40$ , based on an assumed symmetric drift resonance. The drift-resonant interaction is observed to be localized and occur over 5–6 wave cycles, demonstrating peak electron flux modulations at energies  $\sim 60$  keV. Our observation clearly shows electron drift resonance with the fundamental poloidal mode, the energy dependence of the amplitude and phase of the electron flux modulations providing strong evidence for such an interaction. Significantly, the observation highlights the importance of localized wave-particle interactions for understanding energetic particle dynamics in the inner magnetosphere, through the intermediary of ULF waves. **Citation:** Claudepierre, S. G., et al. (2013), Van Allen Probes observation of localized drift resonance between poloidal mode ultra-low frequency waves and 60 keV electrons, *Geophys. Res. Lett.*, 40, 4491–4497, doi:10.1002/grl.50901.

### 1. Introduction

[2] One of the primary goals of the NASA Van Allen Probes mission is to understand the relationship between the various physical processes responsible for energization, transport, and loss of outer radiation belt electrons.

Additional supporting information may be found in the online version of this article.

<sup>1</sup>Space Sciences Department, The Aerospace Corporation, El Segundo, California, USA.

<sup>2</sup>Department of Physics, University of Alberta, Edmonton, Alberta, Canada.

<sup>3</sup>Applied Physics Laboratory, Johns Hopkins University, Laurel, Maryland, USA.

<sup>4</sup>Department of Physics and Astronomy, Dartmouth College, Hanover, New Hampshire, USA.

Corresponding author: S. G. Claudepierre, Space Sciences Department, The Aerospace Corporation, El Segundo, CA, 90245, USA. (seth@aero.org)

©2013. American Geophysical Union. All Rights Reserved. 0094-8276/13/10.1002/grl.50901

Nonadiabatic transport of outer zone electrons is believed to arise mainly from two sources: local acceleration and radial transport. Local acceleration is mediated by resonant wave-particle interactions, where the first adiabatic invariant is violated via gyroresonance between energetic electrons and waves with frequencies commensurate with the electron gyroperiod (e.g., VLF chorus). Radial transport, where the third-adiabatic invariant is violated while conserving the first two, can be roughly subdivided into two categories: prompt acceleration and radial diffusion. Prompt acceleration is a nondiffusive process whereby electrons are coherently accelerated via interaction with ULF waves, the shock-induced compressional wave of the 24 March 1991 event being an extreme case [Li *et al.*, 1993]. On the other hand, radial diffusion results from incoherent scattering in the third invariant, where the rate of diffusion is governed by magnetospheric ULF wave power in the Pc4-5 band. It is becoming increasingly clear that both local acceleration and radial transport play a role in the energization of outer zone electrons to relativistic energies.

[3] Millihertz oscillations in the Earth's magnetic and electric fields are a ubiquitous feature of observations in the magnetosphere, the ionosphere, and on the ground. When such oscillations, known as ULF pulsations, occur in a region of space that is permeated by energetic electrons and/or ions, the ULF waves can potentially interact with the particles. If the ULF waves have appropriate spatial and spectral characteristics, they may resonantly exchange energy with the particles, through a process known as drift resonance [Southwood and Kivelson, 1981]. While it is not entirely clear what drives the ULF wave power necessary to produce radial diffusion in the outer electron belt, a number of studies have identified the solar wind as the potential external source of ULF wave energy [e.g., Mathie and

<sup>5</sup>Institute for the Study of Earth, Oceans, and Space, University of New Hampshire, Durham, New Hampshire, USA.

<sup>6</sup>Space and Atmospheric Sciences Group, Los Alamos National Laboratory, Los Alamos, New Mexico, USA.

<sup>7</sup>Laboratory for Atmospheric and Space Physics, University of Colorado, Boulder, Colorado, USA.

<sup>8</sup>Department of Physics and Astronomy, University of Iowa, Iowa City, Iowa, USA.

<sup>9</sup>Solar System Exploration Division, Goddard Space Flight Center, Greenbelt, Maryland, USA.

<sup>10</sup>Physics Department and Space Science Center, University of New Hampshire, Durham, New Hampshire, USA.

<sup>11</sup>School of Physics and Astronomy, University of Minnesota, Minneapolis, Minnesota, USA.

Mann, 2001]. When averaged over long timescales, it is plausible that the superposition of many impulsive events (e.g., substorm injections, dayside compressions) and/or drift resonance with monochromatic ULF waves can account for the observed correlation between ULF wave power and energetic electron flux in the outer zone [Rostoker et al., 1998], via radial diffusion. Modulations of energetic particle flux via ULF waves have been observed in the Earth's magnetosphere for some time [e.g., Brown et al., 1968]. More recently, in situ event studies have shown some evidence in support of the action of drift resonance, where ULF waves interacting with energetic electrons have been observed by wave and particle instrumentation on the same spacecraft [e.g., Zong et al., 2009]. However, the energy dependence of the amplitude and phase of the electron flux modulations expected from drift resonance theory has been elusive in observations, likely due to sensor limitations in terms of energy, pitch angle and/or spatiotemporal resolution [e.g., Mann et al., The Earth's Van Allen Radiation Belts: Discovery of the Action of A Geophysical Synchrotron, submitted to *Nature Communications*, 2013]. The new capabilities of the NASA Van Allen Probes mission allow us to report here in detail on the first such observations for electron drift resonance with a localized poloidal ULF wave.

## 2. Observations

[4] Figure 1 presents an overview of the interplanetary conditions, geomagnetic activity, and energetic electron flux on 31 October 2012. At this time, the magnetosphere had been in a relatively quiet state following three geomagnetic storms in early October, 2012 (1 Oct, 8 Oct, and 13 Oct). Solar wind speed, solar wind number density, and the  $z_{\text{GSM}}$  component of the interplanetary magnetic field (IMF) are shown in Figures 1a–1c, respectively, from the OMNI 5 min database (i.e., propagated to the bow shock nose). An interplanetary shock impacted the magnetosphere at approximately 15:40:00 UTC. The north-south component of the IMF is weak ( $< 5$  nT), fluctuating around  $B_z = 0$  during the 10 h before the shock arrival, and is predominantly northward afterward. Figures 1d and 1e show the SYM/H and AE indices, respectively, from the OMNI 5 min database. A sudden impulse signature is evident as the sharp rise in SYM/H at the time of the shock arrival and SYM/H is positive during the entire 18 h interval shown. The AE index indicates weak-to-moderate auroral electrojet activity ( $< 300$  nT) that begins around 12:30:00 UTC, prior to the shock arrival. Note that the largest excursion in AE occurs around 14:30:00 UTC, roughly 1 h before the shock arrival, and is associated with an injection of energetic electrons into the inner magnetosphere (see below).

[5] The twin Van Allen Probes spacecraft were launched into a near-equatorial, geotransfer orbit, with apogee near  $L \approx 6$  and contain a comprehensive suite of particle and field sensors designed to study the Earth's radiation environment [Mauk et al., 2012]. Spin-averaged, differential electron flux from the ECT-MagEIS instrument on Van Allen Probe A (henceforth, MagEIS-A) is shown in Figure 1f, for energies 20–600 keV. We refer the reader to the supporting information for more details on the MagEIS instrument. The MagEIS-A data are shown from 14:15:00 to 18:45:00 UTC, a subset of the 18 h OMNI interval shown in Figures 1a–1e. Apogee on spacecraft A occurs at roughly 16:30:00 UTC

near  $L \approx 6$  and  $\text{MLT} \approx 6$ . The magnetic ephemeris calculated from the Olson-Pfizer quiet model [Olson and Pfizer, 1977] are indicated on the horizontal time axis in Figure 1g, which is described in section 3. Note the monochromatic, large amplitude modulations in electron flux that begin around the time of the shock arrival at 15:40:00 UTC and last until about 16:20:00 UTC. The period of these modulations is roughly 3 min ( $f \approx 5.5$  mHz), which places the oscillations in the Pc5 ULF range. It is clear that the amplitude of the flux modulations is largest between 50 and 100 keV, and smaller at energies above and below this range. Flux oscillations at the electron drift-period (i.e., drift-echoes) are also readily apparent for the entire time interval, and in all energy channels shown. These are associated with the substorm injection that occurs prior to the shock arrival, as well as with the arrival of the shock disturbance itself (e.g., Figure 1e), and are discussed in section 3. MagEIS observes electron drift-echoes with surprising regularity and coherency, often following AE enhancements, and this will be the subject of future work. Proton count rate data from MagEIS-A also shows modulations at  $\approx 500$  keV during this interval, though they are longer period oscillations ( $\approx 15$  min) than those observed in the electron data and appear to be drift-echoes. Unfortunately, proton data in the 60–500 keV range from MagEIS-A are unavailable during this event.

[6] Figure 2 presents a summary of wave and particle observations between 15:30:00 and 16:40:00 UTC, encompassing the 3 min period ULF modulation described in Figure 1f. Figure 2a shows the residual electron flux levels from MagEIS-A between 20 and 220 keV. Residual flux is defined as  $\frac{J-J_0}{J_0}$ , where  $J$  is the flux observed in a given MagEIS energy channel (e.g., what is plotted in Figure 1f) and  $J_0$  is a 10 min, running boxcar average of  $J$ . The residual flux is thus a normalized flux level, so that the amplitude of the modulations can be quantitatively compared across the measured energy spectrum. Note that the normalized flux modulations are the strongest in the 57 and 80 keV energy channels and weaker at energies above and below this range. Also, note that there is an apparent phase change in the flux oscillations across the energy range shown. The amplitude and phase of the residual flux oscillations are plotted in Figure 2a, (inset) showing a clear amplitude peak near 57–80 keV (solid trace) with an approximately  $180^\circ$  change in phase (dashed trace) across the amplitude peak. This is a signature of drift resonance [Southwood and Kivelson, 1981] and is elaborated on in section 3.

[7] Magnetic field data from the Van Allen Probe A EMFISIS magnetometer (see the supporting information) are shown in Figure 2b. The EMFISIS magnetic field data are rotated from the GSM coordinate system into a mean-field-aligned (MFA) coordinate system, as described in the supporting information. This decomposition allows the dominant magnetic field wave polarization to be determined as toroidal (azimuthal), poloidal (radial), or compressional (parallel). Figure 2b shows the poloidal component of the magnetic field,  $B_{\text{MFA}}$ , observed on EMFISIS-A. Note the monochromatic ULF oscillations in the poloidal magnetic field at the same frequency as the electron flux modulations between 20 and 200 keV. Vertical dashed traces are shown in all of the panels in Figure 2 and are overlaid at times corresponding to the first six flux amplitude peaks in the MagEIS-A 57 keV channel (Figure 2a). Simultaneous

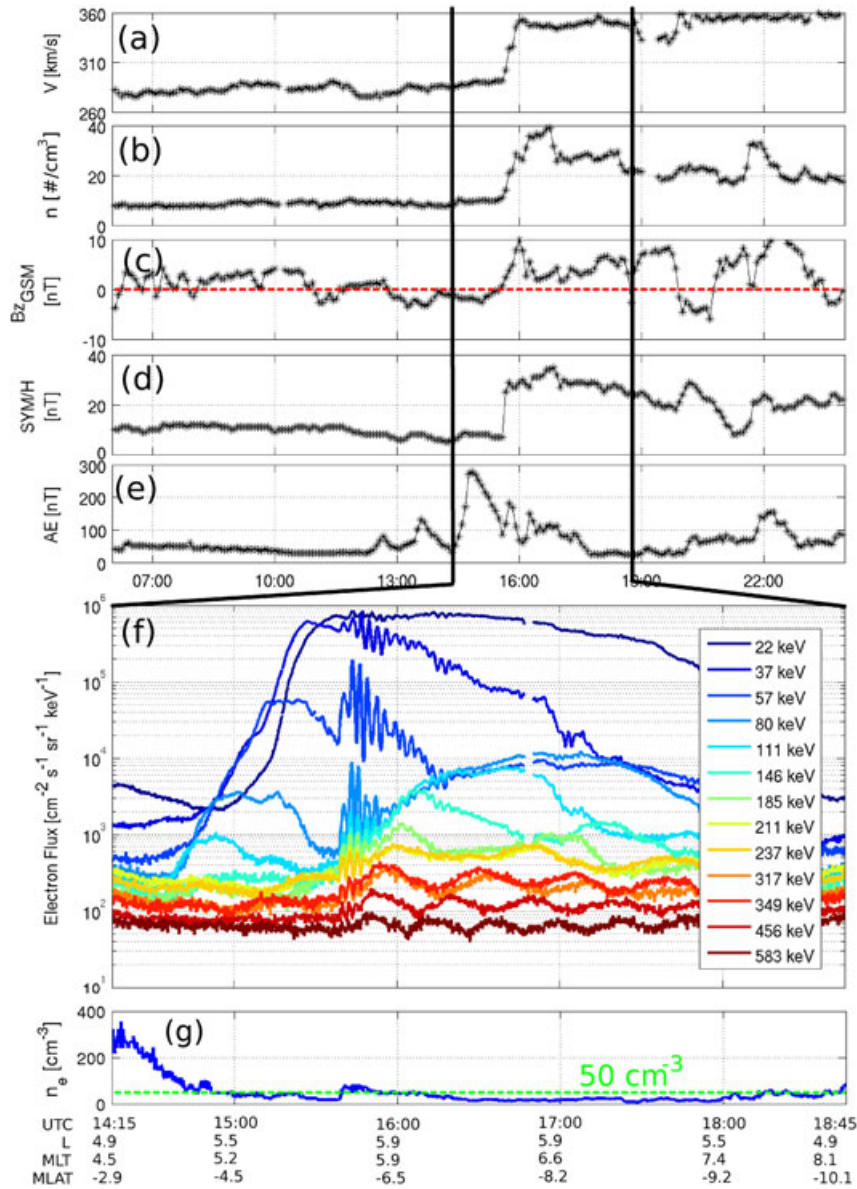


**Figure 1.** Overview of interplanetary conditions, geomagnetic activity, and energetic electron flux on 31 Oct 2012. (a) Solar wind speed, (b) number density, and (c)  $B_{zGSM}$  from the OMNI 5 min database (i.e., propagated to the bow shock nose). (d) SYM/H index and (e) AE index from the OMNI 5 min database. (f) Spin-averaged, differential electron flux from the ECT-MageIS instrument on Van Allen Probe A. (g) Electron number density derived from the upper hybrid line measured by the EMFISIS magnetometer on Van Allen Probe A.

measurements from the Dawson City ground magnetometer station, part of the CARISMA network [Mann *et al.*, 2008], are shown in Figure 2c. Here monochromatic ULF oscillations in the eastward component of the Earth’s magnetic field are observed at the same period as the poloidal ULF magnetic field oscillations observed on EMFISIS-A and the electron flux modulations observed on MagEIS-A. The location of the Dawson City station maps to  $L \approx 6.1$  and MLT  $\approx 5.3$  at 15:45:00 UTC, so that the station is roughly at the foot point of the geomagnetic field line connected to Van Allen Probe A during this event. East-west ground fluctuations map to the poloidal mode in space under the assumption of a  $90^\circ$  polarization rotation for an Alfvén wave upon transmission through the ionosphere. Finally, Figure 2d shows a pitch angle spectrogram from the 80 keV channel

on MagEIS-A. The data are plotted versus local pitch angle, though the magnetic ephemeris in Figure 1 indicates that the Van Allen Probe A spacecraft is  $\lesssim 6^\circ$  off the magnetic equator between 15:30:00 and 16:40:00 UTC. Thus, the local pitch angle is a reasonable approximation of the equatorial pitch angle.

### 3. Discussion

[8] Magnetic and electric field observations from Van Allen Probe A suggest that the observed ULF wave is the fundamental poloidal mode. Figure S1 in the supporting information shows that the 3 min magnetic oscillation observed by EMFISIS-A has strong compressional and radial components, i.e., it is the poloidal mode. We note

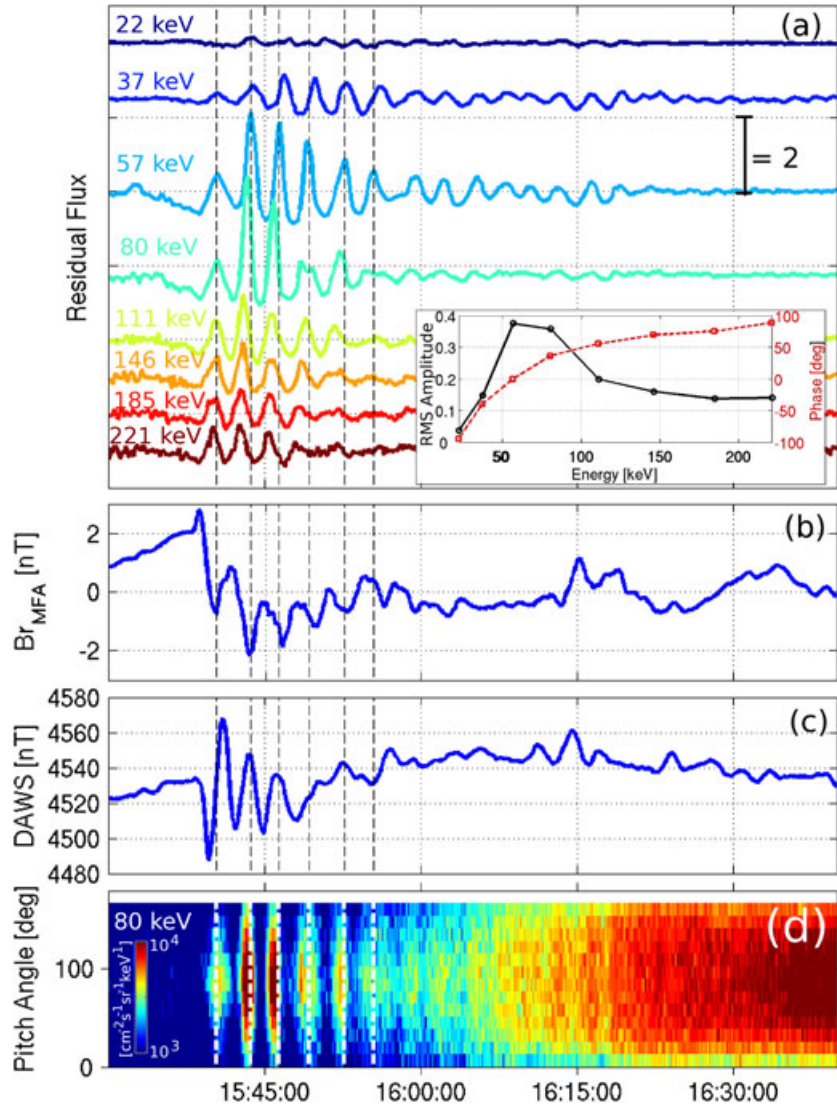


**Figure 2.** Summary of wave and particle observations that suggest drift resonance between magnetospheric ULF waves and energetic electrons. (a) Residual electron flux ( $\frac{J-J_0}{J_0}$ ) from MagEIS-A. (Figure 2a, inset) The amplitude (solid trace) and phase (dashed trace) of the residual flux oscillations. (b) The poloidal component of the magnetic field from the EMFISIS-A magnetometer. (c) East-west component of the Earth’s magnetic field measured at the Dawson City (CARISMA) ground magnetometer station. (d) Pitch angle spectrogram from the 80 keV channel on MagEIS-A.

that magnetospheric ULF waves are never entirely poloidal or toroidal, as the wave modes do not fully decouple in an asymmetric field. The poloidal electric field component,  $E_\phi$ , cannot be reliably measured during this event (see the supporting information). However, ULF electric field oscillations are observed in the two available field components, at the same period as the observed poloidal magnetic field oscillations. Figure 1g shows the profile of the electron number density derived from the EMFISIS-A upper hybrid line during this event. The Van Allen Probe A spacecraft is inside of the dense plasmasphere at the beginning of the time interval shown and moves out of the plasmaspheric region as the spacecraft traverses higher L shells towards apogee. Between 15:45:00 and 16:00:00 UTC, when the poloidal mode ULF wave is observed, we compute the local electron number density to be  $\sim 50 \text{ cm}^{-3}$  (green dashed line in Figure 1g). From this, we estimate the local field line eigen-

frequency in this region of space to be  $\approx 3\text{--}4 \text{ mHz}$  for the fundamental mode, and  $11 \text{ mHz}$  for the second harmonic (see the supporting information). Thus, we conclude that the observed poloidal oscillation is the fundamental mode, as the estimated fundamental mode eigenfrequency is close to the observed wave frequency ( $\approx 5.5 \text{ mHz}$ ). Finally, note that the electron flux oscillations at a fixed energy (e.g., Figure 2d) are independent of pitch angle. This clearly demonstrates that the wave electric field has a symmetric structure about the magnetic equator (i.e., it must be the fundamental mode or an odd harmonic).

[9] The observations presented strongly suggest that the 3 min period flux modulations observed in the 20–500 keV MagEIS channels on Van Allen Probe A are due to drift resonance with the fundamental poloidal mode ULF wave. *Southwood and Kivelson* [1981] developed the general theory of drift-bounce resonance of poloidal ULF waves

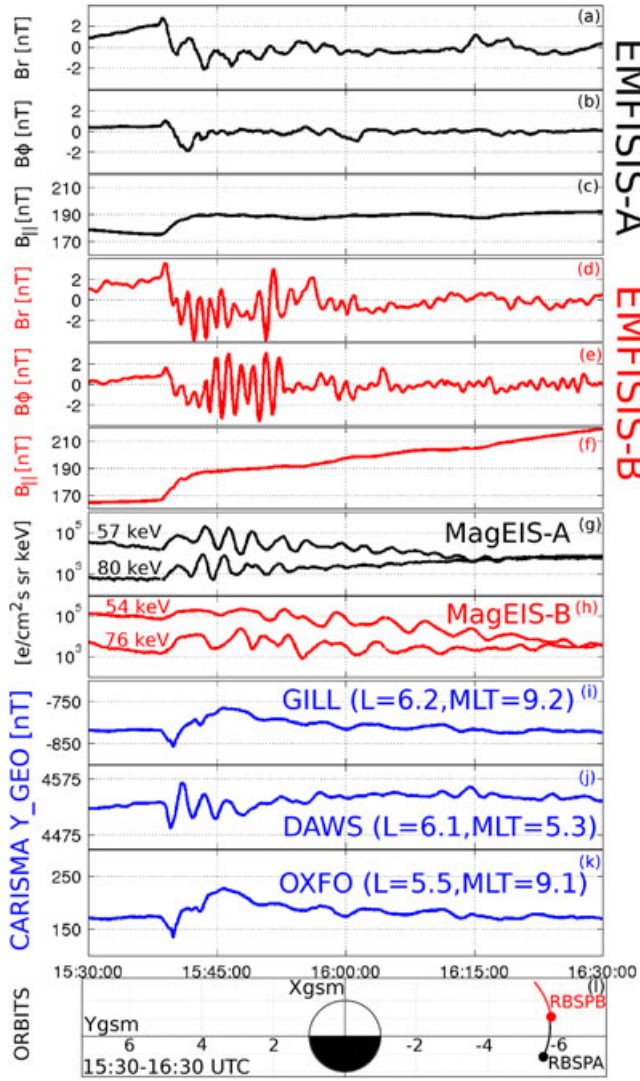


**Figure 3.** Summary of wave and particle observations that suggest a highly localized drift-resonant interaction. Magnetic field from the (a–c) EMFISIS-A and (d–f) EMFISIS-B magnetometers. Electron flux from (g) MagEIS-A and (h) MagEIS-B. East-west component of the Earth’s magnetic field measured at the (i) Gillam, (j) Dawson City, and (k) Oxford House CARISMA ground magnetometer stations. (l) Orbital locations of the Van Allen Probes in the  $xy_{\text{GSM}}$ -plane, from 15:30:00 to 16:30:00 UTC.

with energetic particles. We neglect the bounce motion and focus on the drift resonance, which is a reasonable approximation for typical electron bounce times in this region of space [e.g., Ozeke and Mann, 2008]. In a drift resonant interaction, electron flux oscillations at the resonant energy will be at a maximum, with weaker amplitude flux oscillations at higher and lower energy [Southwood and Kivelson, 1981]. Similarly, electron flux oscillations at the resonant energy will either be in phase or antiphase with the wave electric field ( $E_\phi$ ), and  $90^\circ$  out of phase at higher and lower energy. Both of these features are clear in the residual electron flux oscillations shown in Figure 2a, where a  $180^\circ$  phase shift is observed in the flux oscillations across a peak in amplitude. This strongly suggests that the electrons

are in drift resonance with the fundamental poloidal mode oscillations in  $E_\phi$ . This also suggests that the resonant energy is somewhere between 57 and 80 keV, given the phasing as a function of energy in Figure 2 and the fact that  $E_\phi$  and  $B_r$  should be  $90^\circ$  out of phase for a standing Alfvén wave. Also, as described in Southwood and Kivelson [1981], if an electron drifts at the same rate that the wave moves azimuthally, the electron will see a constant component of the wave field. This is embodied in the well-known drift resonance condition,  $\omega = m\omega_d$ , where  $\omega$  is the ULF wave angular frequency,  $m$  is the azimuthal mode number of the wave and  $\omega_d$  is the angular drift frequency. We estimate the drift frequency of a 60 keV,  $90^\circ$  pitch angle electron drifting at  $L = 5.8$  in a dipole field to be 0.125 mHz [Schulz and Lanzerotti, 1974]. Using this value and the observed value of the wave frequency (5.5 mHz), the drift-resonance condition predicts an azimuthal mode number of  $m = 44$ . This value is consistent with poloidal mode ULF observations and theoretical expectations. We emphasize how much information regarding the ULF waves can be obtained solely from the electron measurements. In this event, we cannot use multispacecraft techniques to estimate the azimuthal wave number because the ULF wave that participates in the drift-resonant interaction is only observed at Van Allen Probe A (see below). For the same reason, the direction of wave propagation cannot be determined in situ for this event. Finally, we note that an alternative explanation for the observed electron flux modulations is the advection by the ULF wave field of a preexisting radial gradient in flux, across the spacecraft position. This seems unlikely, as in this scenario, the flux modulations would all occur in-phase across the measured energy range, and there would not be a peak in the modulation amplitude at a fixed energy.

[10] Figure 3 presents particle and field measurements from both Van Allen Probes spacecraft during this event. The projections of the Van Allen Probes orbits into the GSM equatorial plane are shown in Figure 3l and indicate that the two spacecraft are quite close to one another during this event ( $\lesssim 1$  h of MLT), with spacecraft B leading spacecraft A through apogee between 15:30:00 and 16:30:00 UTC. Magnetic field data from the EMFISIS-A (Figures 3a–3c) and EMFISIS-B (Figures 3d–3f) magnetometers reveal a strikingly different picture of the ULF waves observed during this event. The EMFISIS data are decomposed into MFA coordinates and are shown in the radial (poloidal), azimuthal (toroidal), and parallel (compressional) directions. Note that the 3 min fundamental poloidal mode ULF wave observed at spacecraft A (Figure 3a) is not observed at spacecraft B. A large amplitude, transverse ULF wave is observed by EMFISIS-B, with a frequency  $\approx 12$  mHz, roughly twice that of the poloidal ULF wave observed at spacecraft A, with comparable oscillations in the radial and azimuthal magnetic field components. The transverse wave frequency observed by EMFISIS-B rises with decreasing radial distance, which is consistent with the oscillations being standing Alfvén waves (see the supporting information). We emphasize the dramatic difference between the ULF oscillations observed at spacecraft A versus those at spacecraft B, despite the fact that the two Van Allen Probes are close to one another. Electron flux modulations are observed at MagEIS-B as well (Figure 3h), a few minutes after they are observed at MagEIS-A (Figure 3g), once the interacting electrons have drifted from spacecraft

A to B. MagEIS-B observes these electron flux modulations below  $\approx 200$  keV to be much less coherent than those observed at MagEIS-A (see the supporting information). However, the MagEIS-B flux modulations are coherent and similar to those observed by MagEIS-A above  $\approx 200$  keV. This can be explained by assuming that the drift-resonant interaction occurs over a localized region of space at or near spacecraft A. The lower energy electrons lose their coherency because their drift motion is likely dominated by  $\mathbf{E} \times \mathbf{B}$ -drift, whereas the higher energy electrons remain coherent, as their drift is likely dominated by gradient-curvature-drift. Figures 3i–3k show the east-west component of the geomagnetic field observed at three ground magnetometer stations from the CARISMA network, Gillam, Dawson City, and Oxford House. Note that the ULF wave that participates in the drift-resonant interaction is only observed at the Dawson City station (see the supporting information for additional ground stations). All of these observations suggest that the drift resonance occurs at or near Van Allen Probe A and that the 3 min ULF wave that participates in this interaction is highly localized to this region of space. Finally, note the value of having two Van Allen Probes vehicles in close proximity to one another, which sheds substantial light on the localized nature of the drift resonance.

[11] Oscillations in both the MagEIS-A electron fluxes and the ULF waves are only present for about 5–6 wave periods, which is much less than the electron drift period at these energies. This is likely too few wave cycles for there to be any appreciable transfer of energy between the waves and the electrons, via drift resonance. In addition, the ground-based and in situ observations presented in Figure 3 suggest that the drift-resonant interaction occurs over a localized spatial region near Van Allen Probe A, which also limits the amount of energy which may be transferred between the waves and the particles. Note, however, that large flux increases are observed near the resonant energy (57–111 keV) between 16:00:00 and 17:30:00 UTC, following the drift-resonant interaction (e.g., Figures 1f and 2d). Thus, it may be tempting to conclude that the drift-resonant interaction leads to these flux increases and a net energization of electrons near the resonant energy. Instead, we argue that these flux increases are due to adiabatic effects related to the shock compression of the magnetosphere, combined with the simultaneous presence of drift echoes during this event.

[12] As described in section 2, there is a roughly 300 nT increase in AE around 14:30:00 UTC, coincident with a dispersionless injection of low-energy electrons into the inner magnetosphere (Figure 1e, 1f). After this injection, the electron flux plateaus in the 57–111 keV channels, before falling to near preinjection levels, just prior to the shock arrival. Note that the center of the plateau in the 80 keV channel is at about 15:10:00 UTC. We estimate the drift period of an 80 keV,  $90^\circ$  pitch angle electron drifting at  $L = 5.5$  in a dipole field to be 107 min. Thus, the drift echo in the 80 keV channel should peak around 17:00:00, which is consistent with Figure 1f. Also note that after the shock compression arrives, there are increased fluxes and increased modulation as compared to the echoes that occur before the shock compression (this is true for all energy channels shown, though the preshock echoes are difficult to see in the higher energy channels in Figure 1f, due to the  $y$  axis scale). This might be due to an adiabatic response of the drift-echoing electrons

under the action of the compression. However, the fact that the phase of the drift echoes appears to be reset in the MagEIS energy range suggests a complex interaction incorporating both remnant drift echoes and effects due to the shock arrival. Thus, the observations suggest that the flux increases that are observed between 16:00:00 and 17:30:00 UTC in Figures 1f and 2d, near the resonant energy (57–111 keV), are due to a combination of the shock compression and injection/drift-echo effects. If there is any energization of electrons through drift resonance, it is likely masked by these processes. We emphasize however, that when such drift-resonant interactions are aggregated over a long time interval and over many drift orbits, and occur at multiple isolated locations along the drift orbit, the net effect could produce radial diffusion [e.g., *Elkington et al.*, 2003]. In this event, the drift speed of the modulated particles and duration of the ULF wave, however, preclude the completion of complete drift trajectories for the resonant particles during the interval of wave oscillations. This additionally highlights the potential importance of localized drift-resonant interactions of energetic electrons with poloidal mode waves. Finally, note that even if these adiabatic effects are removed by examining electron phase-space density, effects due to drift echoes are not, and need to be carefully considered.

[13] There are several potential generation mechanisms for the observed fundamental poloidal mode ULF wave. The waves are clearly excited at the time of the shock impact, thus, the standing Alfvén waves could be a direct response to the “ringing” of the magnetosphere. The standard interpretation for the generation of such moderate  $m$ -number poloidal mode ULF waves is drift-bounce resonance with ring current ions [e.g., *Ozeke and Mann*, 2008], though such waves are typically observed in the midnight-to-dusk sector and in the second harmonic. We note that very recent statistical work has suggested that eastward drifting electrons associated with substorm injections can drive poloidal mode ULF waves in the inner magnetosphere [*James et al.*, 2013]. This scenario is consistent with the spatiotemporal ULF wave properties observed and inferred in the present study. In particular, note in Figure 1 that just prior to the shock arrival ( $\sim 15:30:00$  UTC), there is a flattening of the energy spectrum near the resonant energies (80–237 keV). Follow-on work will investigate the possibility that substorm injected electrons themselves can generate poloidal mode ULF waves, via drift resonance.

#### 4. Conclusions

[14] We present Van Allen Probes observations of localized drift resonance between  $\sim 60$  keV electrons and fundamental poloidal mode Pc5 ULF waves, observed near 06 MLT and  $L \approx 6$ . The comprehensive particle and fields instrumentation on the Van Allen Probes allows for a clear, unambiguous identification of the drift-resonant interaction. The impressive energy, pitch angle, and temporal resolution of the MagEIS instrument reveals the energy dependence of the amplitude and phase of the electron flux modulations, which is predicted by drift-resonance theory but has been elusive in past measurements. Moreover, the dramatically different ULF response between the two closely separated Van Allen Probes is striking, and suggests a highly localized interaction. This provides a clean, natural experimental test bed to study ULF wave-particle physics and additional

data from ground magnetometers supports the interpretation of a highly localized drift-resonant interaction. Finally, we emphasize how much information regarding the ULF waves themselves can be inferred solely from high quality, high resolution particle measurements.

[15] **Acknowledgments.** This work was supported by RBSP-ECT funding provided by JHU/APL contract 967399 and EMFISIS funding provided by JHU/APL contract 921647, both under NASA's prime contract NAS5-01072. Work at JHU/APL was supported by NASA grant NNX10AK93G. The OMNI data were obtained from the GSFC/SPDF OMNIWeb interface at <http://omniweb.gsfc.nasa.gov>. CARISMA is operated by the University of Alberta, funded by the Canadian Space Agency. This work is supported in part by participation in the Monitoring, Analyzing and Assessing Radiation Belt Loss and Energization (MAARBLE) consortium. MAARBLE has received funding from the European Community's Seventh Framework Programme (FP7-SPACE-2010-1, SP1 Cooperation, Collaborative project) under grant agreement 284520. This paper reflects only the authors' views and the Union is not liable for any use that may be made of the information contained herein. I.R.M. is supported by a Discovery grant from Canadian NSERC. One author (S.G.C.) would like to thank Jeremy Faden and all of the developers of Autoplot, and Paul O'Brien for making available useful analysis routines.

[16] The Editor thanks two anonymous reviewers for their assistance in evaluating this paper.

## References

- Brown, W. L., L. J. Cahill, L. R. Davis, C. E. McIlwain, and C. S. Roberts (1968), Acceleration of trapped particles during a magnetic storm on April 18, 1965, *J. Geophys. Res.*, *73*(1), 153–161, doi:10.1029/JA073i001p00153.
- Elkington, S. R., M. K. Hudson, and A. A. Chan (2003), Resonant acceleration and diffusion of outer zone electrons in an asymmetric geomagnetic field, *J. Geophys. Res.*, *108*(A3), 1116, doi:10.1029/2001JA009202.
- James, M. K., T. K. Yeoman, P. N. Mager, and D. Y. Klimushkin (2013), The spatio-temporal characteristics of ULF waves driven by substorm injected particles, *J. Geophys. Res. Space Physics*, *118*, 1737–1749, doi:10.1002/jgra.50131.
- Li, X., I. Roth, M. Temerin, J. R. Wygant, M. K. Hudson, and J. B. Blake (1993), Simulation of the prompt energization and transport of radiation belt particles during the March 24, 1991 SSC, *Geophys. Res. Lett.*, *20*, 2423–2426.
- Mann, I. R., et al. (2008), The upgraded CARISMA magnetometer array in the THEMIS Era, *Space Sci. Rev.*, *141*, 413–451, doi:10.1007/s11214-008-9457-6.
- Mathie, R. A., and I. R. Mann (2001), On the solar wind control of Pc5 ULF pulsation power at mid-latitudes: Implications for MeV electron acceleration in the outer radiation belt, *J. Geophys. Res.*, *106*(A12), 29,783–29,796.
- Mauk, B. H., N. J. Fox, S. G. Kanekal, R. L. Kessel, D. G. Sibeck, and A. Ukhorskiy (2012), Science objectives and rationale for the radiation belt storm probes mission, *Space Sci. Rev.*, 1–15, doi:10.1007/s11214-012-9908-y.
- Olson, W. P., and K. A. Pfitzer (1977), Magnetospheric magnetic field modeling, *Tech. Rep.*, Annual Report McDonnell-Douglas Astronautics Co., Huntington Beach, CA.
- Ozeke, L. G., and I. R. Mann (2008), Energization of radiation belt electrons by ring current ion driven ULF waves, *J. Geophys. Res.*, *113*, A02201, doi:10.1029/2007JA012468.
- Rostoker, G., S. Skone, and D. N. Baker (1998), On the origin of relativistic electrons in the magnetosphere associated with some geomagnetic storms, *Geophys. Res. Lett.*, *25*, 3701–3704.
- Schulz, M., and L. J. Lanzerotti (1974), *Particle Diffusion in the Radiation Belts, Physics and Chemistry in Space*, vol. 7, 215 pp., Springer-Verlag, New York.
- Southwood, D. J., and M. G. Kivelson (1981), Charged particle behavior in low-frequency geomagnetic pulsations. I Transverse waves, *J. Geophys. Res.*, *86*, 5643–5655, doi:10.1029/JA086iA07p05643.
- Zong, Q.-G., et al. (2009), Energetic electron response to ULF waves induced by interplanetary shocks in the outer radiation belt, *J. Geophys. Res.*, *114*, A10204, doi:10.1029/2009JA014393.